

# High-Performance OTFTs Using Surface-Modified Alumina Dielectrics

Tommie Wilson Kelley,<sup>\*,†</sup> Larry D. Boardman,<sup>‡</sup> Timothy D. Dunbar,<sup>‡</sup> Dawn V. Muyres,<sup>†</sup> Mark J. Pellerite,<sup>§</sup> and Terry P. Smith<sup>†</sup>

3M Company, 3M Center, Electronics and Inorganic, Interface Materials, and Organic Materials Technology Centers, St. Paul, Minnesota 55144-1000

Received: February 11, 2003; In Final Form: March 24, 2003

We show novel and selective means to modify the dielectric surfaces in organic TFTs. Modification schemes include alkylphosphonic acid monolayers that have a strong affinity for alumina surfaces. Monolayers form robust, extremely uniform thin films and are deposited through simple spin-coating with a dilute solution of the monolayer precursor in solvent. Adding monolayers to organic TFTs has resulted in polycrystalline devices with mobilities nearly equal to single-crystal values while maintaining acceptable values of other device parameters (for example, the threshold voltage, on/off ratio, and subthreshold slope) required for fully functional integrated circuits.

## Introduction

Organic semiconductors have seen wide publicity in potential applications ranging from photoconductors to large-area lighting and low-cost electronics to wallpaper TVs. In recent years, major advances in semiconductor performance<sup>1,2</sup> and organic device construction<sup>3–8</sup> have widened the number of projected applications and heightened the need for research into performance-enhancing treatments<sup>9–12</sup> and processes,<sup>13,14</sup> operational testing,<sup>15</sup> and circuit design<sup>16</sup> suitable for the range of performance seen in organic active materials.

It is widely accepted that polycrystalline films of pentacene, the material with the best thin-film transistor (TFT) performance to date, provide acceptable simple devices under the best preparation conditions and that improved performance, by any definition, may be necessary for the long-term operation of complex organic electronic devices. Well-controlled and optimized conditions result in TFT mobilities for pentacene devices ranging from 0.5 cm<sup>2</sup>/Vs to near the single-crystal mobility, ~3 cm<sup>2</sup>/Vs. High-end performance has been seen sporadically and generally only on test structures with the highest-quality device layers. A recent exception is a report by Infineon of a mobility of 3 cm<sup>2</sup>/Vs for pentacene TFTs with polymeric gate dielectrics.<sup>17</sup>

Some research from Jackson's group<sup>9</sup> has focused on the surface modification of high-quality thermal silicon oxides using organosilanes, resulting in pentacene device constructions with enhanced mobilities. PARC has recently extended this research to cover organosilanes bearing a variety of different terminal groups<sup>12</sup> to investigate the effects of surface energy on the performance of polymeric active layers. The results of these studies have been encouraging in terms of boosting device performance, but ultimately, chemistries are needed that will result in improved performance for lower-cost, more processible dielectrics such as alumina (Al<sub>2</sub>O<sub>3</sub>), which can be applied by plasma-enhanced chemical vapor deposition (PECVD), sput-

tering, or electron beam processes. In addition, alumina has a higher dielectric constant than silica and may provide a route to devices with lower operating voltages.

Our work shows the use of robust chemistry to form uniform, single monolayers on aluminum oxide dielectrics without the likelihood of side reactions and excess deposition that are often observed for silane-based chemistries. These side reactions may result in oligomeric material that is not surface-attached, leaving reactive groups exposed to the sensitive semiconductor–dielectric interface.<sup>18,19</sup> Using phosphonic acid-terminated materials results in stable, high-quality monolayer films without the possibility of side reactions and, once rinsed, without the presence of unbound reactive groups.<sup>20–23</sup> Devices fabricated with pentacene deposited on top of self-assembled monolayers (SAMs) of alkanephosphonic acids display device mobilities rivaling single-crystal results, even in polycrystalline thin films. The chemistry and coating method is quick and facile and would lend itself well to an in-line manufacturing process. Our best results have been found on long (C<sub>12</sub>–C<sub>16</sub>) alkyl chain, methyl-, or phenyl-terminated phosphonic acid monolayers. These results are also general with respect to the organic semiconductor in that performance improvements have been demonstrated for 2,9-dimethylpentacene and could be extended to sexithiophene, tetracene, perylene, and other modified pentacene materials.<sup>24</sup> We believe that this surface treatment method is generalizable to any organic semiconductor that grows with a lamellar or platelike habit and is also general for any aluminum oxide surface where the root-mean-square (rms) roughness is less than the thickness of the subsequently applied monolayer. Furthermore, phosphonic acid SAMs have an affinity for other transition-metal oxides that are widely used in electronic devices such as indium tin oxide (ITO).<sup>20,25–27</sup>

## Materials

Phosphonobenzene (mp 162–165 °C) and 1-phosphonooctane (mp 99–102 °C) were purchased from Aldrich Chemicals and Alfa Aesar, respectively, and were used as received. 1-Phosphonohexadecane was received from Oryza Laboratories as a mixture with the corresponding monoethyl and diethyl esters. A mixture of 5.0 g (approximately 14 mmol) of this material

\* Corresponding author. E-mail: twkelley1@mmm.com. Phone: (651)-733-8314. Fax: (651)-733-2590.

<sup>†</sup> Electronics and Inorganic Technology Center.

<sup>‡</sup> Interface Materials Technology Center.

<sup>§</sup> Organic Materials Technology Center.

and 40 mL of concentrated hydrochloric acid was heated at 100 °C for 12 h. The mixture was diluted with 10 mL of water, and the precipitated solid was collected by filtration. Recrystallization from heptane afforded 3.27 g (76%) of white crystals, mp 95–97 °C. Other phosphonic acids were generally synthesized by a two-step procedure involving the initial reaction of the corresponding bromide or iodide with triethyl phosphite via the Arbuzov reaction.<sup>28</sup> Converting the resulting diethyl phosphonate esters to the free acids was effected in high yield under mild conditions by reaction with bromotrimethylsilane followed by methanolysis of the intermediate silyl ester.<sup>20</sup> The preparation of 1-phosphono-(3*R*/5,7*R*,11*R*)-3,7,11,15-tetramethylhexadecane is typical.

**1-Phosphono-(3*R*/5,7*R*,11*R*)-3,7,11,15-tetramethylhexadecane.** A mixture of 21.69 g (60 mmol) of 1-bromo-(3*R*/5,7*R*,11*R*)-3,7,11,15-tetramethylhexadecane<sup>29</sup> and 25 g (150 mmol) of triethyl phosphite was heated at 150 °C. After 18 h, an additional 20 g (120 mmol) of triethyl phosphite was added, and heating was continued for 24 h. Diethyl ethylphosphonate and other volatiles were distilled (bp 30–50 °C at 0.05 mmHg), and bulb-to-bulb distillation of the concentrate provided 23.51 g (94%) of 1-(diethylphosphono)-(3*R*/5,7*R*,11*R*)-3,7,11,15-tetramethylhexadecane as a clear, colorless liquid, bp 190–230 °C at 0.05 mmHg. To a solution of 14.6 g (35 mmol) of the diethyl phosphonate ester in 40 mL of dichloromethane was added 15.0 g (98 mmol) of bromotrimethylsilane. After 24 h at room temperature, the solution was concentrated to a pale yellowish liquid, and the intermediate silyl phosphonate ester was dissolved in 100 mL of methanol. The resultant solution was stirred at room temperature for 30 min and concentrated to a white solid. Dissolution in methanol and concentration were repeated two times, and recrystallization from ethyl acetate afforded 10.5 g (83%) of 1-phosphono-(3*R*/5,7*R*,11*R*)-3,7,11,15-tetramethylhexadecane as white crystals, mp 69–72 °C. <sup>1</sup>H NMR (CDCl<sub>3</sub>): δ 0.86 (m, 15 H), 1.0–1.5 (m, 22 H), 1.52 (m, 1 H), 1.70 (m, 3 H), 11.12 (br s, 2 H); <sup>13</sup>C NMR (CDCl<sub>3</sub>): δ 18.89, 18.95, 19.52, 19.59, 19.61, 19.65, 19.57, 22.56, 22.66, 22.70 (*J*<sub>CP</sub> = 147 Hz), 24.29, 24.41, 24.73, 27.89, 28.65 (*J*<sub>CP</sub> = 5 Hz), 28.75 (*J*<sub>CP</sub> = 5 Hz), 32.70, 32.71, 33.31 (*J*<sub>CP</sub> = 17 Hz), 36.54, 37.21, 37.31, 37.33, 37.36, 37.38, 37.43, 37.47, 39.29; <sup>31</sup>P NMR (CDCl<sub>3</sub>): δ 38.81; HRMS: calculated for C<sub>20</sub>H<sub>44</sub>O<sub>3</sub>P (M + H<sup>+</sup>) 363.3028, measured 363.3030.

**Methyl 11-Phosphonoundecanoate.**<sup>30</sup> This compound was prepared from methyl 11-bromoundecanoate in 81% overall isolated yield. The final product was obtained as white crystals from a 4:1 mixture of water and 2-propanol, mp 84–88 °C. <sup>1</sup>H NMR (CDCl<sub>3</sub>): δ 1.30 (m, 12 H), 1.60 (m, 4 H), 1.70 (m, 2 H), 2.32 (t, *J* = 6 Hz, 2 H), 3.64 (s, 3 H), 11.01 (br s, 2 H); <sup>13</sup>C NMR (CDCl<sub>3</sub>): δ 21.83, 24.72, 25.13 (*J*<sub>CP</sub> = 145 Hz), 28.81–29.14 (6 C), 30.22 (*J*<sub>CP</sub> = 18 Hz), 33.87, 51.25, 174.16; <sup>31</sup>P NMR (CDCl<sub>3</sub>): δ 32.67; HRMS: calculated for C<sub>12</sub>H<sub>26</sub>O<sub>5</sub>P (M + H<sup>+</sup>) 281.1518, measured 281.1533.

**1-Phosphono-1*H*,1*H*,2*H*,2*H*-perfluorodecane.** This compound was prepared from 1-iodo-1*H*,1*H*,2*H*,2*H*-perfluorodecane in 48% overall isolated yield. The final product was obtained as white crystals from ethyl acetate, mp 170–178 °C. <sup>1</sup>H NMR (*d*<sub>4</sub>-methanol): δ 1.92 (m, 2 H), 2.44 (m, 2 H); <sup>13</sup>C NMR (*d*<sub>4</sub>-methanol): δ 19.55 (d, *J*<sub>CP</sub> = 142 Hz), 26.85 (t, *J*<sub>CF</sub> = 22 Hz); <sup>31</sup>P NMR (*d*<sub>4</sub>-methanol): δ 24.6; HRMS: calculated for C<sub>10</sub>H<sub>6</sub>F<sub>16</sub>O<sub>3</sub>P (M – F<sup>+</sup>) 508.9799, measured 508.9793.

**13-Phenyl-1-phosphonotridecane.** This compound was prepared from 13-phenyl-1-bromotridecane<sup>31</sup> in 83% overall isolated yield. The final product was obtained as white crystals from acetonitrile or hexane, mp 83–86 °C. <sup>1</sup>H NMR (CDCl<sub>3</sub>):

δ 1.24 (m, 18 H), 1.62 (m, 4 H), 1.75 (m, 2 H), 2.60 (t, *J* = 6 Hz, 2 H), 7.20 (m, 5 H), 10.27 (br s, 2 H); <sup>13</sup>C NMR (CDCl<sub>3</sub>): δ 22.26, 25.46 (*J*<sub>CP</sub> = 147 Hz), 29.31, 29.60–29.90 (7 C), 30.69 (*J*<sub>CP</sub> = 18 Hz), 31.78, 36.23, 125.77, 128.44 (2 C), 128.62 (2 C), 143.18; <sup>31</sup>P NMR (CDCl<sub>3</sub>): δ 38.63; HRMS: calculated for C<sub>19</sub>H<sub>34</sub>O<sub>3</sub>P (M + H<sup>+</sup>) 341.2246, measured 341.2240.

**16-Chloro-1-phosphohexadecane.** To a solution of 9.9 g (31 mmol) of 16-bromo-1-hexadecanol in 100 mL of dichloromethane at 0 °C was added 3.1 g (31 mmol) of triethylamine. A solution of 2.9 g (37 mmol) of acetyl chloride in 20 mL of dichloromethane was added dropwise, and the reaction mixture was stirred at 0 °C for 2.5 h. The solution was washed with water until the pH of the aqueous phase was approximately 6, and the organic phase was dried over MgSO<sub>4</sub>. Concentration gave 10.5 g (93%) of crude 1-acetoxy-16-bromohexadecane, which was used without further purification. A mixture of 10.4 g (29 mmol) of the acetoxy derivative and 14.4 g (87 mmol) triethyl phosphite was heated for 48 h at 145 °C. Diethyl ethylphosphonate and other volatiles were distilled (bp 30–50 °C at 0.05 mmHg), and the crude concentrate of 16-acetoxy-1-(diethylphosphono)hexadecane was used without further purification. A mixture of 3.0 g (7 mmol) of the diethyl phosphonate ester and 35 mL of concentrated hydrochloric acid was heated at 100 °C for 9 days. The mixture was diluted with 20 mL of water, and the precipitated solid was collected by filtration. Recrystallization from a 15:1 mixture of heptane and 2-propanol afforded 1.35 g (44%) of 16-chloro-1-phosphohexadecane as a white solid, mp 94–97 °C. <sup>1</sup>H NMR (*d*<sub>8</sub>-tetrahydrofuran): δ 1.23 (m, 20 H), 1.40 (m, 4 H), 1.58 (m, 4 H), 1.74 (m, 2 H), 3.51 (t, *J* = 6 Hz, 2 H), 10.78 (br s, 2 H); <sup>13</sup>C NMR (*d*<sub>8</sub>-tetrahydrofuran): δ 23.70 (*J*<sub>CP</sub> = 4 Hz), 27.78, 27.82 (*J*<sub>CP</sub> = 143 Hz), 29.85, 30.24, 30.46–30.63 (8 C), 31.64 (*J*<sub>CP</sub> = 17 Hz), 33.64, 45.51; <sup>31</sup>P NMR (*d*<sub>8</sub>-tetrahydrofuran): δ 36.25; HRMS: calculated for C<sub>16</sub>H<sub>35</sub>ClO<sub>3</sub>P (M + H<sup>+</sup>) 341.2012, measured 341.2015.

## Sample Preparation

Alumina-coated (1500-Å) Si ⟨100⟩ wafers were obtained from Silicon Valley Microelectronics (San Jose, CA) with an Al gate layer (5000 Å) applied to the back side of each doped wafer. Wafers were quartered and cleaned using consecutive solvent rinses in acetone, methanol, 2-propanol, and water, blown dry in a stream of N<sub>2</sub>, and finally exposed to 5 min of UV/ozone in a home-built chamber. Cleaned quarters were then coated with the SAM of interest by spin-coating a few milliliters of a 0.1 wt % solution of the monolayer precursor in ethanol (500 rpm for 5 s, 2000 rpm for 30 s). Samples were then baked on a vacuum hotplate at 150 °C for 3 min, rinsed with copious amounts of absolute ethanol, and blown dry with a stream of N<sub>2</sub>.

## Sample Characterization

Single-wavelength ellipsometry (Gaertner model L116-A), assuming a refractive index of 1.45 for the monolayers,<sup>31</sup> was performed on each type of monolayer-coated sample. Water contact-angle measurements (AST Products, video contact-angle analyzer, model VCA-2500XE) were also obtained for each type of monolayer. Table 1 shows thickness and static, advancing, and receding water contact-angle (st/adv/rec WCA) data for selected phosphonic acid SAMs studied in this work. The compounds listed in Table 1 represent a wide range of terminal functional groups. Water completely wet the surface of cleaved silica and alumina controls, rendering contact-angle measurements impossible. The proximity of receding contact angle to

**TABLE 1: Thickness and Water Contact-Angle Data of SAMs and Surfaces**

sample	coating thickness (Å)	st/adv/rec WCA
alumina control	N/A	<40/<40/<40
silica control	N/A	<40/<40/<40
13-phenyl-1-phosphonotridecane	17	88/91/79
1-phosphonohexadecane	18	109/116/103
1-phosphono-1H,1H,2H,2H-perfluorodecane	9 <sup>a</sup>	110/121/101
phosphonobenzene	25 <sup>b</sup>	80/85/44
methyl 11-phosphonoundecanoate	N/A	65/72/53
16-chloro-1-phosphonohexadecane	N/A	83/86/79
1-phosphono-(3 <i>R</i> /5 <i>R</i> ,7 <i>R</i> ,11 <i>R</i> )-3,7,11,15-tetramethylhexadecane	14	112/113/100
1-phosphonooctane	10	107/113/101

<sup>a</sup> A refractive index of 1.35 was used to obtain the ellipsometric thickness for monolayers of 1-phosphono-1H,1H,2H,2H-perfluorodecane. <sup>b</sup> The thickness value for phosphonobenzene is higher than that expected for a single monolayer and is attributed to large crystals, observed by AFM, that formed on the surface during the coating process. This was the only coating observed to be nonuniform in film quality.

advancing contact angle is often viewed as an indication of film quality. On the basis of our understanding of the literature and AFM images of phosphonic acid coatings on alumina, the film quality of these samples was excellent, except for films formed from phosphonobenzene. Higher WCA samples gave the best device performance, as detailed in Table 2, with the exception of 1-phosphono-1H,1H,2H,2H-perfluorodecane. Data represented in Table 1 are averages of three measurements on each sample. Silica controls were included in order to compare our work with recent publications whereas alumina controls served as our reference point for comparison with the SAM-coated devices.

AFM (Digital Instruments, Nanoscope IIIa) images were also obtained for bare alumina samples and samples of alumina coated with each monolayer to guarantee uniform coverage and to measure surface roughness. Single-crystal silicon tapping-mode tips were obtained from MikroMasch (NSC12 UL-

TRASHARP cantilevers). Spring constants typically ranged from 4.5 to 14 N/m, and resonant frequencies, from 150 to 310 kHz (manufacturer's specifications). Images were obtained at scan rates of 1–2 Hz at a resolution of 512 lines per image.

Once monolayer-coated samples had been prepared, control samples were prepared using the same series of solvent rinses used for monolayer preparation, followed by 15 min of exposure to UV/ozone to ensure the removal of solvent residue. Control samples and monolayer-coated samples were then placed in a vacuum deposition chamber ( $2 \times 10^{-6}$  Torr), and pentacene (Aldrich, gradient sublimed under flowing  $H_2$  in  $N_2$  to a maximum temperature of 300 °C) was sublimed (260–300 °C) onto the samples as a blanket layer to a final thickness of  $\sim 300$  Å, determined from AFM step-height images, at a rate of 0.1 Å/s. Alternatively, 2,9-dimethylpentacene, synthesized in-house and purified under similar conditions, was sublimed as a blanket layer. Coated samples were moved to a second vacuum chamber ( $2 \times 10^{-6}$  Torr) where Au (600-Å thickness, as measured by a quartz crystal microbalance, QCM) was vapor deposited through a shadow mask to form source and drain contacts. The Al coating on the back side of the doped wafers serves as a field plane gate. Resultant TFTs had dimensions ranging from 40 to 100  $\mu m$  (channel length, L) by 1000  $\mu m$  (channel width, W).

## Device Testing

TFTs were characterized using an HP Semiconductor Parameter Analyzer by sweeping the gate voltage,  $V_g$  (+10 to –40 V), and allowing the drain voltage,  $V_d$ , to remain constant at –40 V. Device traces as shown in Figure 1 were obtained under ambient conditions for at least two separate pentacene depositions on each type of monolayer, and at least three TFTs were measured from each deposition run. Devices fabricated with 2,9-dimethylpentacene were tested in an identical fashion using only a single deposition run.

$I_d^{1/2}-V_g$  and  $I_d-V_g$  traces were used to estimate the saturation mobility ( $\mu$ ), threshold voltage ( $V_t$ ), subthreshold slope ( $S$ ), and on/off ratio. Table 2 shows averaged device properties for the

**TABLE 2: TFT Data for Control and SAM-Coated Surfaces**

sample	$V_t$ (V)	mobility (cm <sup>2</sup> /Vs)	$S$ (V/decade)	on/off	TFTs/dep runs
Pentacene					
alumina control	–6.0	1.1	0.9	$6.1 \times 10^6$	39/6
silica control <sup>a</sup>	–9.4	1.0	1.6	$3.0 \times 10^6$	40/6
13-phenyl-1-phosphonotridecane	–3.2	1.8	0.8	$5.0 \times 10^6$	8/2
1-phosphonohexadecane (exceptional)	–7.8	3.3	2.9	$1.6 \times 10^6$	8/2
1-phosphonohexadecane (overall average)	–5.0	2.0	5.1	$2.4 \times 10^6$	34/10
1-phosphono-1H,1H,2H,2H-perfluorodecane	–3.5	0.4	7.5	$1.5 \times 10^3$	11/3
phosphonobenzene	–4.5	0.1	2.4	$3.6 \times 10^5$	8/2
methyl 11-phosphonoundecanoate	–7.3	0.4	3.8	$3.0 \times 10^6$	9/3
16-chloro-1-phosphonohexadecane	–8.3	0.5	2.3	$4.8 \times 10^5$	11/3
1-phosphono-(3 <i>R</i> /5 <i>R</i> ,7 <i>R</i> ,11 <i>R</i> )-3,7,11,15-tetramethylhexadecane	+5.4	1.8	2.8	$4.5 \times 10^5$	13/3
1-phosphonooctane	–2.1	2.1	2.5	$1.7 \times 10^6$	12/4
2,9-Dimethylpentacene					
alumina control	–3.6	1.1	1.2	$1.3 \times 10^6$	4/1
1-phosphonohexadecane	–3.8	2.5	1.9	$2.0 \times 10^6$	6/1

<sup>a</sup> Silica values differ significantly from the values reported in ref 24 because of the decreased surface roughness of the lot of silica wafers used for this study.



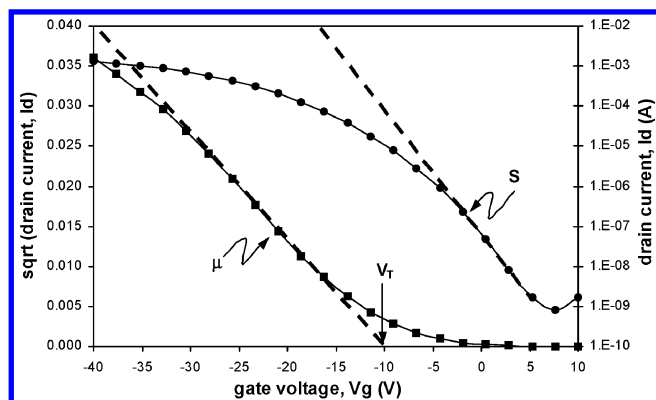


**Figure 1.** Representative TFT trace for pentacene deposited on an alumina sample treated with 1-phosphonohexadecane.  $V_d$  is held constant at  $-40$  V, and  $V_g$  is swept from  $+10$  to  $-40$  V. A linear fit to the  $I_d^{1/2}$ – $V_g$  trace permits the extraction of saturation mobility and threshold voltage ( $V_T$ ) (input parameters are  $W$ ,  $L$ , and the specific capacitance of the oxide),<sup>32</sup> and a linear fit to the  $I_d$ – $V_g$  trace allows us to extract the subthreshold slope ( $S$ ) and the on/off ratio. Device parameters for this sample were  $\mu_{\text{sat}} = 3.4$   $\text{cm}^2/\text{Vs}$ ,  $V_T = -10.4$  V,  $S = 3.4$  V/decade, and on/off =  $1.5 \times 10^6$ . Traces similar to this one for identical voltage excursions were obtained for all of the samples listed in Tables 1 and 2.

same series of monolayers listed in Table 1 for both pentacene and 2,9-dimethylpentacene. All device results are compared with silica and alumina control values. Methyl-terminated and phenyl-terminated alkanephosphonic acid SAMs showed the largest increase in device performance, with improvements of about 200% (and even 300% in some cases) observed for longer alkyl and branched alkyl chains. Devices fabricated with 2,9-dimethylpentacene as the semiconductor also showed a 200–300% improvement in the mobility. Smaller improvements were also observed for other treatments with various chemical terminations and chain lengths. Chlorine- and fluorine-terminated monolayers, decreased the pentacene TFT performance. In general, and in basic agreement with prior work with silane monolayers, high water contact angles ( $80$ – $115^\circ$ ) resulted in the largest performance increase. A slight increase in the subthreshold slope was observed for most of these surface treatments.<sup>33</sup> Currently, we do not have independent control of device parameters, but other materials and methods are under investigation toward this end. The fluorinated phosphonic acid monolayers, despite high WCAs, gave lower mobility. This suggests that chemistry as well as surface energy may be important in device performance. Low WCAs ( $40$ – $80^\circ$ ) also appeared to decrease device performance. Additionally, preliminary results on sexithiophene devices indicate that the interaction of heteroatoms in the semiconductor with the surface treatment may also play a role. The data represented in Table 2 are averaged over the total number of TFTs measured in several pentacene depositions. This is indicated in the last column of the Table, where the total number of TFTs measured over the number of deposition runs included in the TFT count is indicated (e.g., the alumina control data can be interpreted as 39 individual transistors sampled over 6 separate pentacene deposition runs). Typically, four TFTs were measured on each sample. Two entries are listed for 1-phosphonohexadecane. The exceptional values occurred over two deposition runs where every TFT tested on each sample behaved with a mobility near  $3$   $\text{cm}^2/\text{Vs}$ . A larger number of deposition runs for the same surface coating (including the exceptional runs) gives an average device mobility of  $2$   $\text{cm}^2/\text{Vs}$ .

AFM images (Figure 2) of very thin ( $10$ – $75$  Å) layers of pentacene deposited on these monolayer coatings seem to

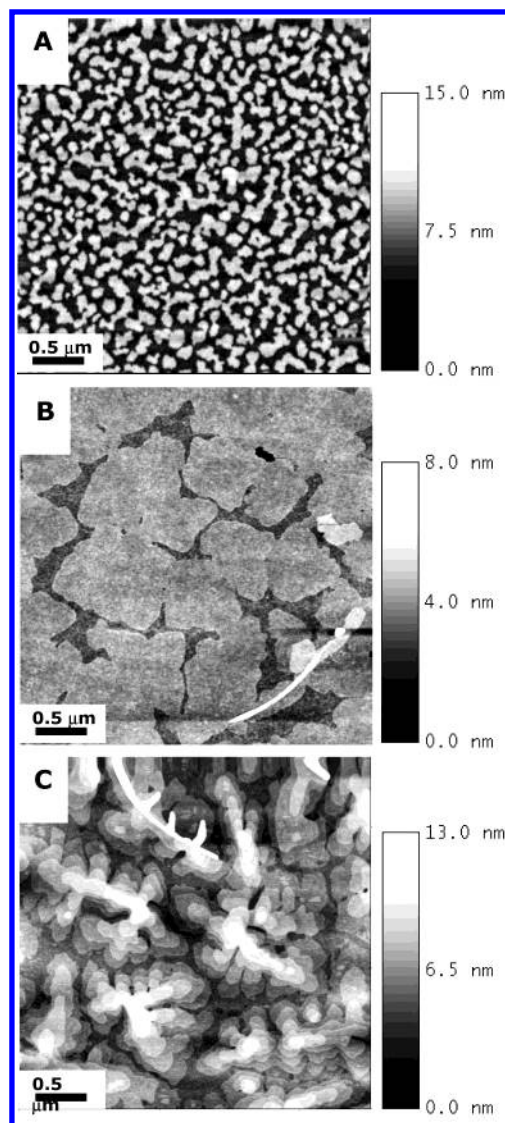


**Figure 2.** AFM images of 1-phosphonohexadecane with increasing coverage of pentacene. Bright areas in the images are interpreted as increasing film thickness in the  $z$ , or out-of-plane, direction. This series can be interpreted as snapshots of film growth. The thickness of these ultrathin layers was estimated using a QCM. (A) Initial stages ( $10$ -Å coverage) show a large number of nucleation sites and some lateral growth with no growth in the vertical direction. (B) With increasing coverage ( $35$  Å), a second layer of material is nucleated on top of the first layer as the first layer continues to fill in laterally (lateral growth  $\gg$  vertical growth). (C) With further pentacene deposition ( $75$  Å), the vertical growth rate seems to more nearly equal the rate of lateral growth in that several incomplete layers are manifested as lamellae in the pentacene grains.

indicate that sharp, well-defined grain boundaries are not present in the first few full monolayers of pentacene high-performance films. This could explain our near single-crystal pentacene mobilities in that the interfacial phosphonic acid SAM enables the formation of several molecular layers of near single-crystal-quality pentacene.<sup>34</sup> X-ray diffraction results of deposited films of pentacene (thickness  $\sim 300$  Å) indicate that we generally have films composed primarily of the thin-film phase ( $d$  spacing =  $15.1$  Å) with small fractions of the bulk phase present. By controlling the surface chemistry, we provide a smooth, passivated surface on which pentacene can grow, improving the crystallinity in the early stages of pentacene film growth. The result is a polycrystalline device in which the first few molecular layers have been engineered to give behavior approaching that

of a bulk, single-crystal device. It is widely believed that most of the charge transport in organic TFTs occurs in the first few monolayers of the semiconductor; therefore, the quality of these layers may very well determine the ultimate mobility as well as other relevant performance characteristics of the devices.

## Summary

High-performance pentacene devices have been reliably fabricated using phosphonic acid-treated alumina dielectrics. Results indicate that both chemistry and surface energy play important roles in determining device performance. Furthermore, monolayers can be integrated into fully patterned device structures because of the affinity of phosphonic acids for alumina. Initial results show that these monolayers reduce the effective surface roughness on an electron beam-deposited oxide (rms roughness  $\sim 1\text{--}2\text{ nm}$ ).<sup>35</sup> Chain length appears to be a major factor in optimizing the performance of rough oxides with these coatings and needs to be carefully investigated to realize equivalent improvements in fully patterned devices. If the chain is too short, then the oxides may not be fully passivated because of disorder in the coatings. Research continues in this area to find other useful forms of surface modification as well as to track the shelf life and operational stability of these devices. Additionally, research is underway to develop surface modification methods that provide independent control of device parameters (e.g., treatments that would provide a mobility of 2 and might allow one to change the threshold voltage from a positive to a negative value). Low-temperature, high-vacuum measurements and studies of the effects of surface roughness are also in progress in collaboration with the University of Minnesota.

## Conclusions

We present here a survey of a method<sup>24</sup> that may be applied to create enhanced performance in organic semiconductor devices through the use of phosphonic acid chemistry to attach SAMs to relevant device oxides such as aluminum oxide. The coatings appear to provide a smooth, noninteracting surface on which the semiconductor can grow with near single-crystal quality for the first few full monolayers. Pentacene devices treated with 1-phosphonohexadecane have shown a 300% improvement in mobility over untreated control devices, and other phosphonic acid SAMs have reliably resulted in 200% improvement without sacrificing acceptable values for other important device parameters. In addition, this method has been applied to show similar improvements in the performance of devices fabricated with 2,9-dimethylpentacene and shows promise for other organic semiconductors including tetracene, perylene, and sexithiophene. Continuing research includes the integration of these and other surface treatment methods into devices fabricated with low-temperature materials and processes (for example, polymeric substrates and electron beam-deposited oxides).<sup>36</sup>

**Acknowledgment.** Special thanks to Dennis and Kim Vogel of 3M for their efforts in the synthesis and purification of 2,9-dimethylpentacene.

## References and Notes

- (1) Dimitrakopoulos, C. D.; Purushothaman, S.; Kymissis, J.; Callegari, A.; Shaw, J. M. *Science* **1999**, *283*, 822.
- (2) Dimitrakopoulos, C. D.; Mascaro, D. J. *IBM J. Res. Dev.* **2001**, *45*, 11.
- (3) Ullmann, A.; Ficker, J.; Fix, W.; Host, H.; Clemens, W.; McCulloch, I.; Giles, M. *Mater. Res. Soc. Symp. Proc.* **2001**, *665*, C7.5.2.
- (4) Gelinck, G. H.; Geuns, T. C. T.; de Leeuw, D. M. *Appl. Phys. Lett.* **2000**, *77*, 1487.
- (5) Necliudov, P. V.; Shur, M. S.; Gundlach, D. J.; Jackson, T. N. *J. Appl. Phys.* **2000**, *88*, 6594.
- (6) Klauk, H.; Gundlach, D. J.; Nichols, J. A.; Jackson, T. N. *IEEE Trans. Electron Devices* **1999**, *46*, 1258.
- (7) Klauk, H.; Jackson, T. N. *Solid State Technol.* **2000**, *63*.
- (8) Sirringhaus, H.; Kawase, T.; Friend, R. H.; Shimoda, T.; Inbasekaran, M.; Wu, W.; Woo, E. P. *Science* **2000**, *290*, 2123.
- (9) Gundlach, D. J.; Kuo, C. C.; Nelson, S. F.; Jackson, T. N. *DRC Conf. Dig.* **1999**, 164.
- (10) Shtein, M.; Mapel, J.; Benziger, J. B.; Forrest, S. R. *Appl. Phys. Lett.* **2002**, *81*, 268.
- (11) Swiggers, M. L.; Xia, G.; Slinker, J. D.; Gorodetsky, A. A.; Malliaras, G. G.; Headrick, R. L.; Weslowski, B. T.; Shashidhar, R. N.; Dulcey, C. S. *Appl. Phys. Lett.* **2001**, *79*, 1300.
- (12) Salleo, A.; Chabiny, M. L.; Yang, M. S.; Street, R. A. *Appl. Phys. Lett.* **2002**, *81*, 4383.
- (13) Chabiny, M. L.; Wong, W. S.; Salleo, A.; Paul, K. E.; Street, R. A. *Appl. Phys. Lett.* **2002**, *81*, 4260.
- (14) Halik, M.; Klauk, H.; Zschieschang, U.; Kriem, T.; Schmid, G.; Radlik, W.; Wussow, K. *Appl. Phys. Lett.* **2002**, *81*, 289.
- (15) Knipp, D.; Street, R. A.; Volkel, A.; Ho, J. J. *Appl. Phys.* **2003**, *93*, 347.
- (16) Baude, P. F.; Ender, D. E.; Kelley, T. W.; Haase, M. A.; Muryes, D. V.; Theiss, S. *Appl. Phys. Lett.*, in press.
- (17) Klauk, H.; Halik, M.; Zschieschang, U.; Schmid, G.; Radlik, W. *J. Appl. Phys.* **2002**, *92*, 5259.
- (18) Wasserman, S. R.; Tao, Y.-T.; Whitesides, G. M. *Langmuir* **1989**, *5*, 1074.
- (19) Maoz, R.; Sagiv, J. *J. Colloid Interface Sci.* **1984**, *100*, 465.
- (20) Gardner, T. J.; Frisbie, C. D.; Wrighton, M. S. *J. Am. Chem. Soc.* **1995**, *117*, 6927.
- (21) Van Alsten, J. G. *Langmuir* **1999**, *15*, 7605.
- (22) Folkers, J. P.; Gorman, C. B.; Laibinis, P. E.; Bucholz, S.; Whitesides, G. M. *Langmuir* **1995**, *11*, 813.
- (23) Messerschmidt, C.; Schwartz, D. K. *Langmuir* **2001**, *17*, 462.
- (24) Kelley, T. W.; Muryes, D. V.; Pellerite, M. J.; Dunbar, T. D.; Boardman, L. D.; Smith, T. P. U.S. Patent 6,433,359, 2002.
- (25) Gao, W.; Dickinson, L.; Grozinger, C.; Morin, F. G.; Reven, L. *Langmuir* **1996**, *12*, 6429.
- (26) Appleyard, S. F. J.; Willis, M. R. *Opt. Mater.* **1998**, *9*, 120.
- (27) Goetting, L. B.; Deng, T.; Whitesides, G. M. *Langmuir* **1999**, *15*, 1182.
- (28) Bhattacharya, A. K.; Thyagarajan, G. *Chem. Rev.* **1981**, *81*, 415.
- (29) Sita, L. R. *J. Org. Chem.* **1993**, *58*, 5285.
- (30) Boutevin, B.; Piétrasanta, Y.; Rigal, G. *Makromol. Chem.* **1982**, *183*, 2347.
- (31) Lee, S.; Puck, A.; Graupe, M.; Colorado, R.; Shon, Y.-S.; Lee, T. R.; Perry, S. S. *Langmuir* **2001**, *17*, 7364.
- (32) The dielectric constant of the aluminum oxide film was taken to be the ideal value, giving a specific capacitance of  $0.000448\text{ pF}/\mu\text{m}^2$ . Measured specific capacitances were somewhat lower than this value, typically  $0.000345\text{ pF}/\mu\text{m}^2$ . The ideal value was used throughout this study to obtain conservative estimates of the mobility. Sequential scans of the same TFT and other TFTs on the same sample showed no shifts in  $V_t$  or mobility, an indication that the effects of the slow charging/discharging of the dielectric layer were minimal.
- (33) It has been brought to our attention that increases in the subthreshold slope may be due to impurities from the SAM layers influencing the interface between the semiconductor and dielectric. Extensive purification and comparison were beyond the scope of this project but could lead to a broader control of device performance.
- (34) Laquindanum, J. G.; Katz, H. E.; Lovinger, A. J.; Dodabalapur, A. *Chem. Mater.* **1996**, *8*, 2542.
- (35) Literature results have correlated reduced surface roughness with increased mobility in TFTs. See, for example, ref 15 herein.
- (36) Kelley, T. W.; Muryes, D. V.; Pellerite, M. J.; Dunbar, T. D.; Boardman, L. D.; Smith, T. P.; Jones, T. D.; Baude, P. F. *Mater. Res. Soc. Symp. Proc.* **2003**, submitted for publication.